Magnetic "Dead" Layer at a Complex Oxide Interface

Weidong Luo,[1,2,*] Stephen J. Pennycook,[2] and Sokrates T. Pantelides[1,2]

[1]*Department of Physics and Astronomy, Vanderbilt University, Nashville, Tennessee 37235, USA*

[2]*Materials Science and Technology Division, Oak Ridge National Laboratory, Oak Ridge, Tennessee 37831, USA*

(Received 20 May 2008; published 10 December 2008)

Recent magnetic measurements at $La_{0.67}Ca_{0.33}MnO_3/YBa_2Cu_3O_7$ interfaces led to conflicting interpretations: a magnetic "dead" layer on the LCMO side or antiparallel Cu and Mn magnetic moments. Here we report results of first-principles density-functional calculations of position-dependent magnetic couplings between interlayer and intralayer Mn atoms. The couplings in the first few layers near the interface are found to be weak ferromagnetic or even antiferromagnetic. The results suggest that a "dead" magnetic layer 2–3 atoms thick is present, as needed to account for the observations.

DOI: 10.1103/PhysRevLett.101.247204 PACS numbers: 75.70.Cn, 71.15.Mb, 75.10.Hk

Transition metal oxides (TMOs) have a broad range of physical properties. Electron- and hole-doped cuprates such as $YBa_2Cu_3O_{7-\delta}$ (YBCO) are high-T_c superconductors. $BaTiO_3$ and related compounds are ferroelectrics. Several properties of TMOs depend on parameters such as dopant density, temperature, and external pressure [1]. For example, the mixed-valance manganite $La_xCa_{1-x}MnO_3$ (LCMO) system has a complex phase diagram [2]. Depending on the doping concentration x, it can be a ferromagnetic (FM) metal exhibiting colossal magnetoresistance, an antiferromagnetic (AFM) insulator with charge and orbital ordering, or a paramagnetic insulator.

Additional phenomena arise when one makes interfaces or superlattices by connecting together two different TMOs. Examples are depression of superconductivity in YBCO in a superlattice with ferromagnetic LCMO [3,4], suppression of free carrier density [5], and reconstruction of orbital occupation and orbital symmetry [6]. Theoretical studies with model Hamiltonians have led to conclusions about charge transfer and orbital reconstruction behavior at a superconductor-ferromagnet (SC-FM) interface [7,8] due to Fermi level mismatch at the two sides of the interface. TMO superlattices also exhibit special magnetic properties: a magnetic coupling between $La_{0.67}Sr_{0.33}MnO_3$ (LSMO) layers in a LSMO/YBCO/LSMO superlattice [9] and depression of the saturation magnetization in the LCMO/YBCO superlattices [10].

In this work, we focus on the magnetic properties of LCMO/YBCO superlattices, with doping $x = 0.67$ in LCMO. In 2005, Stahn *et al.* [11] reported neutron reflectometry data and proposed two different possible explanations in terms of two different magnetization profiles: (a) a magnetic "dead" layer with zero net magnetic moment in LCMO near the LCMO/YBCO interface, and (b) a magnetic moment on Cu in YBCO antiparallel to the one in LCMO. Shortly thereafter, Hoffmann *et al.* reported data that supported option (a) [12], while Chakhalian *et al.* reported data that supported option (b) [13]. In addition, Hoffmann *et al.* found a large reduction of the saturation magnetization in the middle of the LCMO layer. Although magnetic "dead" layers in transitional metal interfaces are often attributed to chemical interdiffusion [14,15], electron microscopy observations have concluded that there is no major chemical intermixing across the LCMO/YBCO interface [16]. The quandary has remained unresolved.

In this Letter, we report the results of extensive density-functional theory (DFT) investigations of the magnetic properties of a LCMO/YBCO superlattice. We used these results to extract values for local intralayer and interlayer magnetic couplings. We find that the LCMO layers adjacent to YBCO have small values of either FM or AFM coupling, while layers farther from the interface exhibit strong FM coupling, similar to the bulk LCMO. The result is a clear signature of a magnetic "dead" layer in LCMO that arises simply by the presence of the interface with YBCO, without the need to involve any particular magnetic properties in the latter.

DFT [17,18] calculations in the generalized-gradient approximation were performed using plane-wave basis set and the projector-augmented-wave method [19] as implemented in the Vienna *ab initio* simulation package (VASP) code [20]. The calculations were performed on the -YBCO-LCMO-YBCO- superlattice using supercells containing 6–9 layers of LCMO and 3 units of YBCO (each YBCO unit contains 1 CuO chain and 2 CuO_2 planes). The structures of the LMCO and the YBCO are based on experimental orthorhombic unit cells [21,22]. The doping level in LCMO is simulated using regular arrangements of 2:1 ratio of La to Ca atoms in the appropriate sublattice. The interfacial CuO chains in YBCO are missing and replaced by MnO_2 planes [16]. The in-plane lattice constants of LCMO and YBCO are matched to construct perfect superlattices. Because of the computational cost, most of the calculations are performed with the perfect superlattices without further relaxations of the structure. Atomic relaxation at the interface is not expected to be large. We are in the region of pseudomorphic growth. Furthermore, electron microcopy observations indicate

 © 2008 The American Physical Society

that atomic displacements at the interface are less than 0.1 Å [16]. In addition, we performed test calculations that allow atomic relaxations of the interfacial Mn-O layer while keeping fixed the positions of all other atoms.

DFT is known to produce excellent ground-state properties. In a recent work, it was shown that DFT yields excellent predictions for the structural, electronic, and magnetic-ordering properties of LCMO across a range of doping [23]. Collinear spin polarizations are employed in the calculations for various possible magnetic configurations of Mn atoms. Electronic iterations are carried out to obtain self-consistent results, from which the total energies, orbital occupancies of Mn atoms, and magnetic configurations are obtained. In TMOs, it is not practical to let the electronic self-consistency calculation determine the ground-state magnetic ordering because of the following reasons: (a) the total energy differences between different magnetic phases, such as FM and AFM, are small; (b) energy barriers in the magnetic configuration space generally exist between (meta)stable magnetic phases. Rather, the total energies from DFT calculations of various magnetic orderings, such as FM, *G*-type AFM, *A*-type AFM, and *C*-type AFM, are compared, and the magnetic ground state is obtained by choosing the lowest energy configuration. In bulk $La_{2/3}Ca_{1/3}MnO_3$, FM ordering is found to have the lowest energy compared to various AFM orderings, in agreement with experimental data [2].

Because bulk LCMO has a FM ground state at the composition we considered, we begin our calculations by assuming FM spin configuration of LCMO in the superlattice. We first consider a supercell with 6 layers of LCMO and 3 layers of YBCO. The self-consistent results from DFT show parallel Mn spin directions, with a small reduction of Mn magnetic moments at the interface, as plotted in Fig. 1. The magnetization in the LCMO part of the superlattice is close to the corresponding bulk values. Obviously, this type of magnetic configuration does not explain the magnetic profile of a magnetic "dead" layer in LCMO. Calculations performed with a larger supercell containing 9 LCMO layers give essentially the same results, i.e., a small reduction of Mn magnetic moments next to the interface.

The orbital occupancies of Mn $3d$ e_g states in the FM superlattice are plotted in Fig. 2. Near the interface, the Mn e_g occupancies are reduced from their bulk values. The small reduction of orbital occupancy is consistent with the small dip in the interface magnetic moments. However, the magnetic *coupling* between a pair of neighboring Mn spins may change drastically when the orbital occupancies are reduced. In bulk LCMO, Mn $3d$ orbital occupancy is controlled by varying the doping, resulting in FM or AFM ground-state orderings with very different magnetic couplings [2]. The reduction of Mn $3d$ orbital occupancy near the interface indicates a possibility that the local magnetic interactions near the interface are different from the bulk value, and the first few LCMO layers next to YBCO may not have FM ordering.

In order to probe further, we performed a series of calculations in which the magnetic ordering of the first two layers was constrained as shown in Table I. In each case we calculated the total energies using DFT and then modeled the resulting differences in terms of a nearest-neighbor Heisenberg model. Both the intralayer and interlayer magnetic energies involving Mn pairs in the first two layers of the interface are modeled with position-dependent coupling strengths J_{ij}. The magnetic energy E_{ij} between Mn sites i and j is modeled as $E_{ij} = J_{ij}\mathbf{S}_i \cdot \mathbf{S}_j$, where $\mathbf{S}_i$ and $\mathbf{S}_j$ are unit vectors along the directions of magnetic moments i and j. From the total energies of these spin configurations, the magnetic interactions involving Mn spins in the first two layers can be extracted. The intralayer magnetic interactions are $J_1 = 0.4$ meV, $J_2 = 2.1$ meV, and interlayer magnetic interactions $J_{12} = -1.7$ meV, $J_{23} = 7.7$ meV.

It is instructive to plot the magnetic interactions as a function of Mn positions to the interface, as is shown in

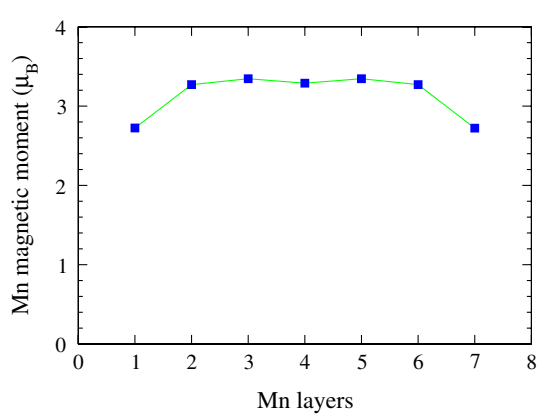

FIG. 1 (color online). Magnetic moment profile of Mn atoms in the LCMO/YBCO superlattice.

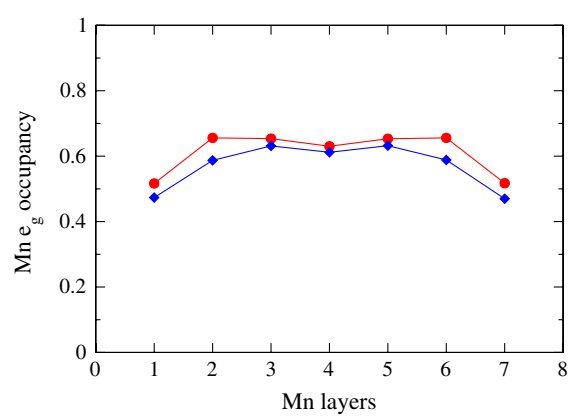

FIG. 2 (color online). Orbital occupancy profile of Mn $3d$ e_g states in the LCMO/YBCO superlattice. The two curves indicate occupancies of the two e_g orbitals.

TABLE I. The various magnetic configurations of Mn spins within the first two layers near the interface in the LCMO/YBCO superlattice, and their relative total energies. Vertical line (|) indicates the interface, plus sign (+) indicates spin-up Mn site, and minus sign (−) indicates spin-down Mn site.

Magnetic configurations	$\vert + + + + \cdots$ $\vert + + + + \cdots$	$\vert + + + + \cdots$ $\vert - + + + \cdots$	$\vert + - + + \cdots$ $\vert - + + + \cdots$	$\vert - + + + \cdots$ $\vert - + + + \cdots$	$\vert + - + + \cdots$ $\vert + - + + \cdots$
Relative energy (meV)	0	−0.6	27.7	−6.9	23.8

Fig. 3. For comparison, the calculated FM coupling in bulk $La_{2/3}Ca_{1/3}MnO_3$ is around 16 meV. Within the first interfacial Mn-O layer in the superlattice, the intralayer FM interaction is very weak. Thermal excitation at a low temperature can destroy the FM ordering. The interlayer magnetic interaction between the first and the second Mn-O layers at the LCMO/YBCO interface prefers antiferromagnetic configuration (negative magnetic interaction in the plot), which would have vanishing total magnetization due to cancellation of up and down magnetic moments in the layers. The weak FM interaction and the appearance of AFM interaction at the interface obtained from our calculations support option (a): a magnetic "dead" layer in LCMO near the LCMO/YBCO interface. Concerning the effects of the atomic relaxation on the magnetic interaction at the interface, we performed test calculations that relax the interfacial Mn-O layer while keeping the rest of the superlattice fixed. The results show that the first two magnetic couplings (the intralayer coupling within the first layer and the interlayer coupling between the first and the second layers) behave essentially the same way. In fact, both magnetic couplings become slightly AFM, while the magnetic couplings farther away from the interface are FM. The picture of magnetic "dead" layer at the interface remains unchanged.

In conclusion, we studied the magnetic properties of LCMO/YBCO superlattice structure using the DFT method. Position-dependent magnetic coupling strengths between interlayer and intralayer Mn atoms are extracted from self-consistent total energy calculations. Even though magnetic coupling in bulk LCMO is FM, the magnetic couplings near the LCMO/YBCO interface become very weak and some of the couplings become AFM. The reduced FM couplings and the appearance of AFM couplings in LCMO near the interface support the existence of a magnetic "dead" layer in LMCO near the LCMO/YBCO interface. The affected magnetic couplings are within 2–3 layers from the interface, in agreement with experimental observation.

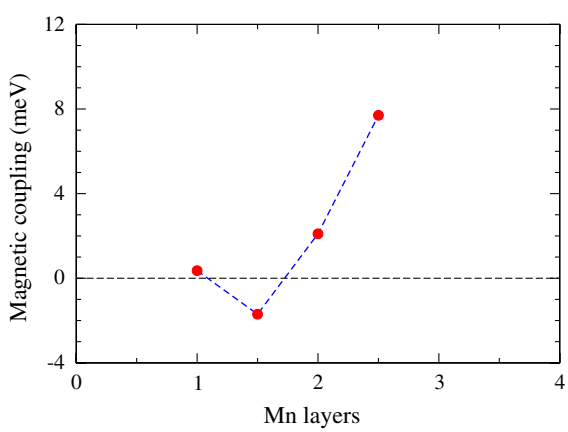

FIG. 3 (color online). Magnetic coupling strengths between intralayer and interlayer Mn atoms at the LCMO/YBCO interface. The couplings at integer positions, such as 1 and 2, are the intralayer couplings, while the interlayer couplings are plotted at half-integer positions, such as 1.5 and 2.5.

Research sponsored in part by the Division of Materials Sciences and Engineering, Office of Basic Energy Sciences, U.S. Department of Energy, under Contract No. DE-AC05-00OR22725 with Oak Ridge National Laboratory, managed and operated by UT-Battelle, LLC, and by the McMinn Endowment at Vanderbilt University. Computations were performed at the National Energy Research Scientific Computing Center.

*Corresponding author.
weidong.luo@vanderbilt.edu

[1] E. Dagotto, Science **309**, 257 (2005).
[2] P. Schiffer, A. P. Ramirez, W. Bao, and S.-W. Cheong, Phys. Rev. Lett. **75**, 3336 (1995).
[3] Z. Sefrioui, D. Arias, V. Peña, J. E. Villegas, M. Varela, P. Prieto, C. León, J. L. Martinez, and J. Santamaria, Phys. Rev. B **67**, 214511 (2003).
[4] Z. Sefrioui, M. Varela, V. Peña, D. Arias, C. León, J. Santamaría, J. E. Villegas, J. L. Martínez, W. Saldarriaga, and P. Prieto, Appl. Phys. Lett. **81**, 4568 (2002).
[5] T. Holden, H.-U. Habermeier, G. Cristiani, A. Golnik, A. Boris, A. Pimenov, J. Humlíček, O. I. Lebedev, G. Van Tendeloo, B. Keimer, and C. Bernhard, Phys. Rev. B **69**, 064505 (2004).
[6] J. Chakhalian, J. W. Freeland, H.-U. Habermeier, G. Cristiani, G. Khaliullin, M. van Veenendaal, and B. Keimer, Science **318**, 1114 (2007).
[7] B. K. Nikolić, J. K. Freericks, and P. Miller, Phys. Rev. B **65**, 064529 (2002).
[8] S. Yunoki, A. Moreo, E. Dagotto, S. Okamoto, S. S. Kancharla, and A. Fujimori, Phys. Rev. B **76**, 064532 (2007).
[9] P. Przyslupski, I. Komissarov, W. Paszkowicz, P. Dluzewski, R. Minikayev, and M. Sawicki, Phys. Rev. B **69**, 134428 (2004).

[10] P. Prieto, P. Vivas, G. Campillo, E. Baca, L. F. Castro, M. Varela, C. Ballesteros, J. E. Villegas, D. Arias, C. León, and J. Santamaría, J. Appl. Phys. **89**, 8026 (2001).
[11] J. Stahn, J. Chakhalian, C. Niedermayer, J. Hoppler, T. Gutberlet, J. Voigt, F. Treubel, H.-U. Habermeier, G. Cristiani, B. Keimer, and C. Bernhard, Phys. Rev. B **71**, 140509(R) (2005).
[12] A. Hoffmann, S. G. E. te Velthuis, Z. Sefrioui, J. Santamaria, M. R. Fitzsimmons, S. Park, and M. Varela, Phys. Rev. B **72**, 140407(R) (2005).
[13] J. Chakhalian, J. W. Freeland, G. Srajer, J. Strempfer, G. Khaliullin, J. C. Cezar, T. Charlton, R. Dalgliesh, C. Bernhard, G. Cristiani, H.-U. Habermeier, and B. Keimer, Nature Phys. **2**, 244 (2006).
[14] Y.-h. Liu, X.-d. Ma, and L.-m. Mei, Phys. Rev. B **45**, 10 459 (1992).
[15] M. Kowalewski, W. H. Butler, N. Moghadam, G. M. Stocks, T. C. Schulthess, K. J. Song, J. R. Thompson, A. S. Arrott, T. Zhu, J. Drewes, R. R. Katti, M. T. McClure, and O. Escorcia, J. Appl. Phys. **87**, 5732 (2000).
[16] M. Varela, A. R. Lupini, S. J. Pennycook, Z. Sefrioui, and J. Santamaria, Solid-State Electron. **47**, 2245 (2003).
[17] P. Hohenberg and W. Kohn, Phys. Rev. **136**, B864 (1964).
[18] W. Kohn and L. J. Sham, Phys. Rev. **140**, A1133 (1965).
[19] P. E. Blöchl, Phys. Rev. B **50**, 17 953 (1994).
[20] G. Kresse and J. Furthmüller, Phys. Rev. B **54**, 11 169 (1996).
[21] A. Williams, G. H. Kwei, R. B. Von Dreele, A. C. Larson, I. D. Raistrick, and D. L. Bish, Phys. Rev. B **37**, 7960 (1988).
[22] Q. Huang, A. Santoro, J. W. Lynn, R. W. Erwin, J. A. Borchers, J. L. Peng, K. Ghosh, and R. L. Greene, Phys. Rev. B **58**, 2684 (1998).
[23] W. Luo, A. Franceschetti, M. Varela, J. Tao, S. J. Pennycook, and S. T. Pantelides, Phys. Rev. Lett. **99**, 036402 (2007).